

See discussions, stats, and author profiles for this publication at: <https://www.researchgate.net/publication/359293027>

Satellite observed vegetation dynamics and drivers in the Namib sand sea over the recent 20 years

Article in *Ecohydrology* · March 2022

DOI: 10.1002/eco.2420

CITATIONS

0

READS

109

2 authors:



[Na Qiao](#)

Indiana University-Purdue University Indianapolis

9 PUBLICATIONS 72 CITATIONS

[SEE PROFILE](#)



[Lixin Wang](#)

Indiana University-Purdue University Indianapolis

276 PUBLICATIONS 7,730 CITATIONS

[SEE PROFILE](#)

Some of the authors of this publication are also working on these related projects:



The physiological effects of periodic water stress in some riparian trees of Namibian ephemeral rivers [View project](#)



Non-rainfall water in the Namib Desert [View project](#)

RESEARCH ARTICLE

WILEY

Satellite observed vegetation dynamics and drivers in the Namib sand sea over the recent 20 years

Na Qiao | Lixin Wang

Department of Earth Sciences, Indiana University-Purdue University Indianapolis (IUPUI), Indianapolis, Indiana, USA

Correspondence

Lixin Wang, Department of Earth Sciences, Indiana University-Purdue University Indianapolis (IUPUI), 723 W Michigan St, SL 118M, Indianapolis IN 46202, USA.
Email: lxwang@iupui.edu

Funding information

National Science Foundation, Grant/Award Number: EAR-1554894

Abstract

Monitoring dryland vegetation trends and examining the drivers are of great importance to understand the dryland vegetation response to future climate changes. Recent findings through satellite data indicate that vegetation greenness has increased in several regions worldwide. These greening patterns are driven by human activities or combined human activities and environmental factors. However, the analyses of greenness trend for regions without direct human activities and shrub expansion in drylands are still lacking. To this end, this study investigates the vegetation trend across the Namib sand sea over March 2000 to December 2018 using monthly Normalized Difference Vegetation Index (NDVI) and examines several potential drivers including precipitation, temperature and atmospheric CO₂ concentration. For the NDVI time series across the whole study region, a significant greening trend was found over March 2000 to September 2012 based on Mann-Kendall test but not over the whole study period. Structural equation modelling results indicated that precipitation and CO₂ were the dominant drivers of greening. Temperature showed negative effects on vegetation greenness, indicating warming would reduce plant growth in the study region. Spatially, 75% of the region showed statistically significant greening over March 2000 to September 2012 and 39.30% for March 2000 to December 2018. The different vegetation trend results between the entire region and the pixel scale implied that location-specific greening could be masked by an overall trend. Our study suggested that precipitation (especially the large episodic precipitation events) and CO₂ are dominant drivers of the observed greening in the Namib. Our findings fill an important knowledge gap of vegetation dynamics in regions without direct human activities.

KEYWORDS

drylands, greening, MODIS NDVI, the Namib Desert, TRMM

1 | INTRODUCTION

Analyses of vegetation trends and the drivers could help tackle future climate change issues because of the important role vegetation plays

in terrestrial ecosystems, atmospheric processes as well as the carbon and water cycles (Bonan et al., 1992; D'Odorico et al., 2010; Griscom et al., 2017; Lanning et al., 2019; Wang et al., 2014). Satellite observation provides the suitable approach for monitoring long-term

This is an open access article under the terms of the Creative Commons Attribution-NonCommercial License, which permits use, distribution and reproduction in any medium, provided the original work is properly cited and is not used for commercial purposes.

© 2022 The Authors. *Ecohydrology* published by John Wiley & Sons Ltd.

vegetation trends at regional and global scales (e.g., Jiao, Wang, & McCabe, 2021; Jiao, Wang, Smith, et al., 2021). There have been reports of significant increasing trends in satellite-derived vegetation proxies (e.g., the Normalized Difference Vegetation Index [NDVI], the Enhanced Vegetation Index [EVI] and the Leaf Area Index [LAI]), commonly regarded as the greening phenomenon, observed in several regions worldwide (Fensholt et al., 2012; Liu et al., 2013; Zhu et al., 2016). Based on an ensemble of LAI datasets during 1982–2009, over 50% of the global vegetated lands (e.g., southeast North America, the northern Amazon, Europe, Central Africa and Southeast Asia) displayed greening trends in growing season, driven by multiple drivers, such as CO₂ fertilisation, climate factors and land cover changes (Zhu et al., 2016). Chen et al. (2019) found that greening occurred in 34% of global vegetated area in the past two decades (2000–2017) using satellite-derived vegetation data. According to this result, China and India account for nearly one-third of the observed greening area mainly due to direct human activities, including afforestation programmes in China (Piao et al., 2015) and increasing harvested area through multiple cropping in both countries (Ambika et al., 2016; Chen et al., 2019). Moreover, unlike these greening regions affected by direct human activities, greening trends were also observed in dryland areas with low influences of human activities (Fensholt et al., 2012; Helldén & Tottrup, 2008), such as the Sahel (Herrmann et al., 2005; Olsson et al., 2005; Pausata et al., 2020), and southern Africa (Saha et al., 2015; Tian et al., 2017).

Dryland ecosystems cover about 40% of the global land surface (Lal, 2004; Wang et al., 2012) and have significant impacts on the livelihoods of approximately more than 1.8 billion people (Gilbert, 2011). Quantifying the spatiotemporal vegetation trend in dryland areas and understanding its causes are therefore important. A few studies have investigated the vegetation greening trend in southern Africa driven by combined effects of climate factors and plant community composition changes (e.g., shrub encroachment) (Saha et al., 2015; Tian et al., 2017; Yu & D'Odorico, 2014). Some findings suggest that a consistent trend of increasing vegetation greenness in the Sahel region was attributed to increasing rainfall, land-use change and migration (Herrmann et al., 2005; Olsson et al., 2005). However, the analyses of regional-scale greening patterns in drylands without the direct influences of human activities and plant community composition changes are still lacking. In these dryland areas, the vegetation greenness changes are only driven by environmental factors such as CO₂, precipitation and temperature.

Examining the drivers of vegetation greening is of great importance to understanding possible land degradation and improving global carbon cycle model (Piao et al., 2020). Greening trends in drylands have been broadly attributed to increased water availability, increased atmospheric CO₂, plant composition changes and land-use changes (Fensholt et al., 2013; Hickler et al., 2005; Lu & Wang, 2019; Lu, Wang, & McCabe, 2016; Olsson et al., 2005; Saha et al., 2015). Particularly, human-related factors, such as migration and grazing practice, are important local drivers of vegetation greenness changes in drylands. However, for the drylands not impacted by these human activities and plant composition changes, such as the Namib sand sea,

the contributions of environmental factors to greening remain ambiguous. Estimating the greening trend in drylands without the direct anthropogenic forcing could help us understand the baseline vegetation dynamics under the ongoing climate changes, improving the reliability of future projected changes in vegetation. Even though some studies reported the greening pattern at a global scale (Piao et al., 2020; Zhu et al., 2016), the spatial patterns and temporal dynamics of vegetation greenness in the Namib sand sea and its reasons have not been investigated in the literature. To this end, the specific objectives of this study are to (1) investigate the vegetation trend across the sand dune portion of the Namib Desert using satellite remote sensing data from the high-quality Moderate Resolution Spectroradiometer (MODIS) product over 2000 to 2018 and (2) examine several potential environmental driving factors (i.e., precipitation, temperature and CO₂) of the observed vegetation trend.

2 | MATERIALS AND METHODS

2.1 | Study area

Since the focus of this study is drylands without the effects of direct human activities and shrub encroachment, we limit our study in the sand dune portion of the Namib Desert (Figure 1). The climate in the Namib Desert is arid and has one wet season (October to April) and one dry season (May to September) (Lu, Wang, Pan, et al., 2016). The typical vegetation species in this region are herbaceous plants, such as *Stipagrostis sabulicola*, *Trianthema hereroensis*, *Stipagrostis gonatostachys*, *Stipagrostis lutescens*, *Stipagrostis ciliata*, *Centropodia glauca* and *Claradoraphis spinosa*. The spatial resolution of study area boundary pixel is 0.25° in accordance with the lowest spatial resolution of remote sensing data used in this study.

2.2 | Datasets

2.2.1 | Vegetation greenness data

There are many satellite-derived vegetation proxies, such as NDVI and EVI, that have been extensively used to monitor and analyse the vegetation greenness and productivity in drylands. There are other remote sensing products to present vegetation attributes, such as LAI or Gross Primary Production (GPP). Based on our pre-analysis, remote sensing products of LAI and GPP are not suitable in this study because of the poor quality of these data attributed to low vegetation coverage in the study area (Pfeifer et al., 2012). Furthermore, both NDVI and EVI show good performances in representing the vegetation dynamics in the study area (Qiao et al., 2020). This study focused on NDVI, to analyse long-term vegetation trends in the study region. The NDVI data were derived from a high-quality MODIS product MCD43A4 (Schaaf & Wang, 2015), providing the daily nadir and bidirectional reflectance distribution function adjusted reflectance bands including MODIS spectral bands 1–7 at 500-m resolution

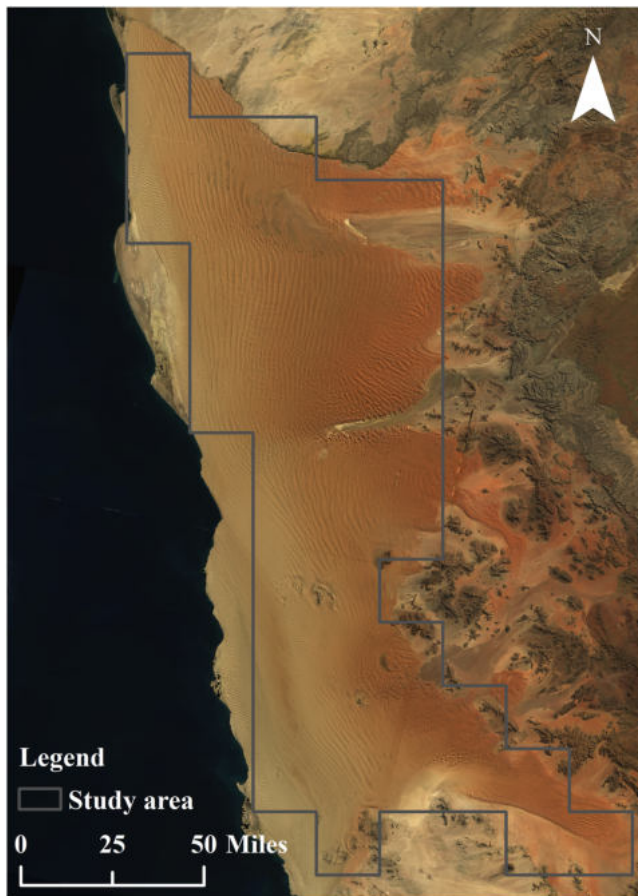


FIGURE 1 Map indicating the sand dune portion of the Namib Desert. The background scene is a natural colour (bands 4, 3 and 2) Landsat 8 composite (February to June 2020)

(<https://lpdaac.usgs.gov/products/mcd43a4v006/>). We extracted this product covering from the first complete month with available daily MODIS images in March 2000 through December 2018 to calculate NDVI. The NDVI pixels were quality filtered by good quality flags according to the associated quality information product (MCD43A2). The daily NDVI data, passed the quality screening, were then resampled into a monthly scale by averaging all valid NDVI value (temporal average).

2.2.2 | Climate data and atmospheric CO₂ concentration data

Since the study area is without the effects of direct human activities and shrub encroachment, the potential driving factors of vegetation greenness trends are mainly associated with environmental factors, such as precipitation, temperature and CO₂.

The precipitation data used in this study were acquired from Tropical Rainfall Measuring Mission precipitation product (TRMM 3B43) (TRMM, 2011) (https://disc2.gesdisc.eosdis.nasa.gov/opensap/TRMM_L3/TRMM_3B43.7/). This product provides average monthly precipitation rates with a spatial resolution of 0.25°. The temperature

data were obtained from the European Centre for Medium Range Weather Forecasts reanalysis dataset (ERA5) (Muñoz Sabater, 2019) (<https://cds.climate.copernicus.eu/cdsapp#!/dataset/reanalysis-era5-land-monthly-means>). The monthly average air temperature at 2-m height with 0.25° spatial resolution provided by ERA5 was used in this study. The spatial resolution of these climate data is lower than that of vegetation greenness data used in this study.

The global monthly mean CO₂ concentration data averaged over marine surface sites, provided by the Global Monitoring Division of National Oceanic and Atmospheric Administration (NOAA) Earth System Research Laboratory (<https://www.esrl.noaa.gov/gmd/ccgg/trends/global.html>) (Ballantyne et al., 2012), were used in this study.

2.3 | Data analyses

We first analysed the long-term vegetation greenness trend on a regional scale for the whole study area. Temporal trends in monthly average MODIS NDVI for the study area were evaluated by the Thiel-Sen estimate of linear slope with Mann-Kendall test, which is a nonparametric rank test to detect monotonic trends (Chen et al., 2019; Sen, 1968; Theil, 1950). The function 'zyp.trend.vector' with Yue-Pilon prewhitening method in R package 'zyp' was applied to conduct the Mann-Kendall test. We also estimated the significant time series shifts ('breakpoints') ($p < 0.05$) in the monthly mean NDVI time series from March 2000 to December 2018 using the R package 'strucchange'. The vegetation greenness trend analyses during the two segments separated by the breakpoint were also investigated by the Mann-Kendall test.

Then, a structural equation model (SEM) (Grace, 2006) was employed to examine the effects of precipitation, air temperature and atmospheric CO₂ concentration on NDVI trend from March 2000 to December 2018 over the study area. SEM is a comprehensive statistical approach to test the structural relationship among observed and latent variables (Hoyle, 1995). SEM statistics were calculated using International Business Machines (IBM) SPSS AMOS version 26. A maximum likelihood based goodness-of-fit test in SEM was used to assess the degree of accord between observed and predicted covariance structures (Grace, 2006). The calculated path coefficients, one of the output parameters of SEM, are based on the amount of variance explained in the response variables and they represent relative strengths of the specific pathways (e.g., Eldridge et al., 2015; Lu, Wang, & McCabe, 2016). Here, the path coefficients refer to the corresponding effects of environmental factors on vegetation changes. Another output parameter of SEM, R^2 value, represents the total variance explained by all of the contributing variables including precipitation, temperature and CO₂. Before conducting the SEM, we used windowed cross-correlation (WCC) method (Boker et al., 2002) to analyse the potential time-lag between vegetation greenness and precipitation at a monthly scale (Table S1). The results showed that vegetation had a 2-month lag response to precipitation. To remove the lag effects of precipitation to vegetation growth, the time series of precipitation data was moved forward by 2 months compared with

these time series of other studied variables. The SEM was also conducted for each segment study period separated by the breakpoint.

To investigate the spatial pattern of greenness trend in the study area, we performed the Mann–Kendall statistical analyses on the pixel scale using the MODIS monthly mean NDVI dataset at a 500-m spatial resolution in the study region. This study especially focused the heavy precipitation effects on greening using statistics of annual extreme precipitation amount and the number of extreme precipitation events. The extreme precipitation event is defined as precipitation amount above the 95% quantile of all precipitation data during a reference period (Seveviratne et al., 2012). Here, we used all available monthly precipitation data in TRMM 3B43 from 1980 to 2018 as the reference period to calculate the 95% quantile. The month with precipitation amount above the 95% quantile was counted as an extreme precipitation event. The annual frequency of extreme precipitation events is calculated by the number of months with extreme precipitation divided by 12.

3 | RESULTS

3.1 | Trends in NDVI time series across the whole study region

Figure 2 shows the temporal dynamics of all the studied variables from March 2000 to December 2018 for the whole study region. There is no consistently seasonal change in NDVI time series of the study area (Figure 2). According to the NDVI time series, vegetation greenness in the study region generally experienced a phase of gradual increasing from 2000 to 2012 and then decreased until 2016. Nonsignificant vegetation trend in the NDVI time series of the study area during the entire study period was detected. We used breakpoint analysis to obtain the breakpoint timing in the NDVI time series. The result showed a significant breakpoint in September 2012. Based on the breakpoint result, we then investigated the NDVI trends before the breakpoint (March 2000 to September 2012), after the break

point (October 2012 to December 2018) and the entire study period with Mann–Kendall test.

Significant greening trend in the study region was found during the first segment (March 2000 to September 2012) before the breakpoint based on Mann–Kendall test using monthly mean NDVI time series (Figure 2), and the Theil–Sen slopes is 0.00006 NDVI unit month⁻¹ ($p < 0.05$). There were no significant vegetation greenness trends indicated by Mann–Kendall test during the second segment and the entire study period.

For the first segment, there were three pronounced peak values of NDVI at around 2006, 2008 and 2012, which were roughly in accordance with the timing of peak values in precipitation, observed by the simple moving average curves (Figure 2). Moreover, the mean annual precipitation amount after the breakpoint was significantly lower than that before the breakpoint ($p < 0.01$, Mann–Whitney–Wilcoxon test), but temperature did not show significant difference before and after the breakpoint. These results implied that the significant shift in the NDVI time series was related to the precipitation variability before and after the breakpoint. For the overall trends of environmental factors, atmospheric CO₂ concentration with the feature of seasonal cycle showed significant increasing trends during both segments and the entire study period using Mann–Kendall test, while no significant trends were found in temperature and precipitation time series in any segment or the entire study period.

3.2 | Relationships between NDVI trends and climatic drivers

In order to evaluate the contributions of precipitation, air temperature and atmospheric CO₂ concentration to greening trend in the study region, three SEMs were set up based on the two segments before (March 2000 to September 2012) and after the breakpoint (October 2012 to December 2018) as well as the entire study period (Figure 3). The input data of SEM include the time series of precipitation, air temperature, atmospheric CO₂ concentration and NDVI (Figure 2). For the first segment, SEM results show that the effect of CO₂ concentration on vegetation greenness (path coefficient = 0.60) was stronger than that of precipitation (path coefficient = 0.31). This result indicated that CO₂ had the dominant contribution to the greening trend for the first segment in the study region. Temperature showed the negative effects on greenness (path coefficient = -0.31), with the same absolute value to the path coefficient of precipitation. Regarding the second segment from October 2012 to December 2018, precipitation exhibited a positive effect on the NDVI trend (path coefficient = 0.40), both temperature and CO₂ concentration showed negative effects on vegetation trend (path coefficient = -0.39 for temperature and path coefficient = -0.22 for CO₂). For the entire study period, both precipitation and CO₂ concentration had positive effects on greening in this region (path coefficient = 0.38 for precipitation and path coefficient = 0.23 for CO₂). Temperature presented the similar negative effects on

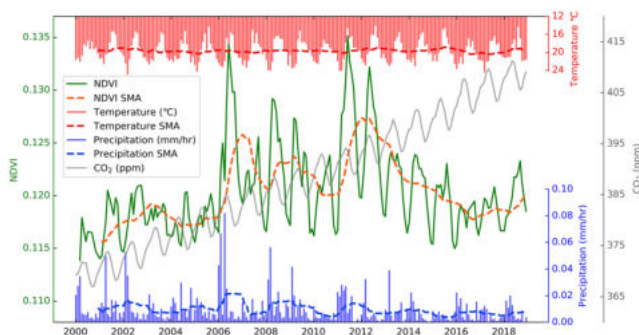


FIGURE 2 Monthly mean time series of Normalized Difference Vegetation Index (NDVI), precipitation rate, air temperature and atmospheric CO₂ concentration from March 2000 to December 2018 for the study region outlined in Figure 1. SMA refers to simple moving average with a window size of 12 months

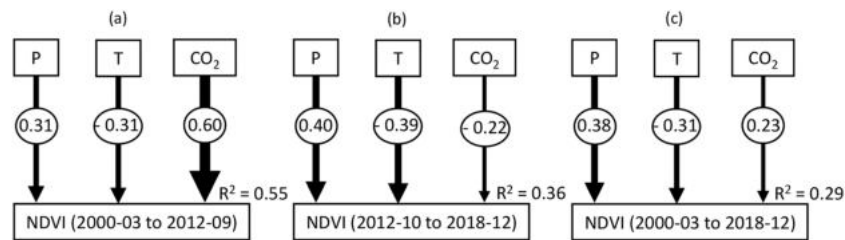
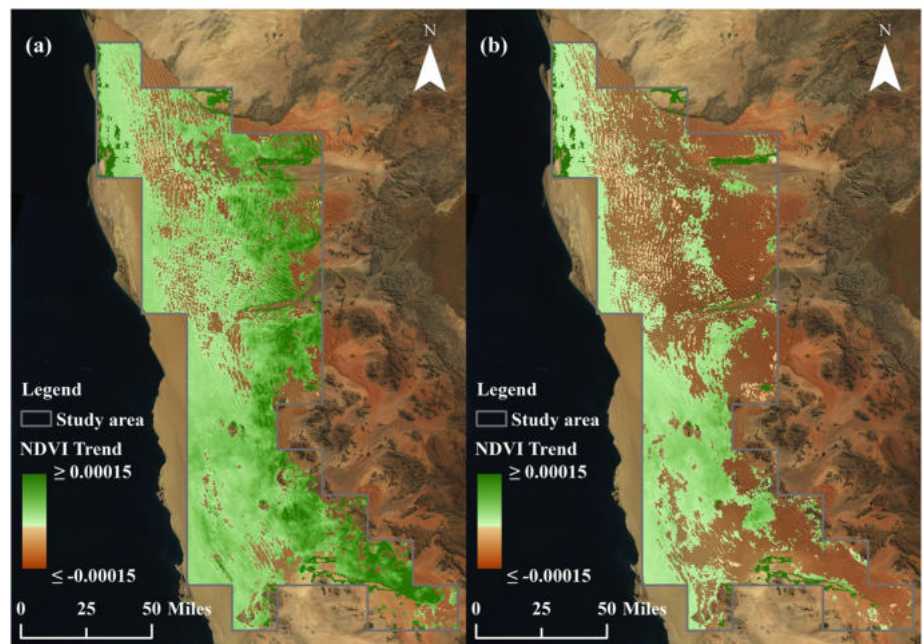


FIGURE 3 Structural equation modelling of the effects of precipitation (P), air temperature (T) and atmospheric CO₂ concentration (CO₂) on greenness (Normalized Difference Vegetation Index [NDVI]) for the study area. Relationships between NDVI and potential drivers in March 2000 to September 2012, October 2012 to December 2018 and the entire study periods were shown in panels (a), (b) and (c), respectively. Arrow thickness is proportional to path coefficient

FIGURE 4 Spatial distribution patterns of vegetation trends in monthly average Moderate Resolution Spectroradiometer (MODIS) Normalized Difference Vegetation Index (NDVI) covering March 2000 to September 2012 (a) and March 2000 to December 2018 (b) in the study area. Pixels with statistically significant trends (Mann–Kendall test, $p < 0.1$) are colour coded. The unit of vegetation trend is NDVI \times month⁻¹



vegetation trend during the first segment and the entire study period (path coefficient = -0.31). These results indicate that precipitation performed the consistent positive effects on greenness across the study periods, whereas the temperature effects were negative. This result reveals that warming could reduce vegetation growth in this study area. The effect of CO₂ concentration on greenness was positive when the vegetation presented significant greening trend, while CO₂ effects for the periods without significant vegetation trends were not consistent.

3.3 | Spatial patterns of vegetation greenness trends

To better understand vegetation greening pattern observed in the study region, we evaluated the spatial distribution of trends in monthly averaged NDVI during March 2000 to September 2012 and the entire study period using the Mann–Kendall test. Figure 4 illustrates the spatial extent of significant vegetation trends at a 500-m

resolution. The trends with $p < 0.1$ were considered to be statistically significant (Chen et al., 2019), and there was similar pattern at $p < 0.05$. About 74.79% of the study region exhibited significant greening trend over March 2000 to September 2012; the value was 39.30% for the entire study period. Only 0.67% was characterised by significantly negative trends over March 2000 to September 2012 and 3.33% for the entire study period. The average pixel-level NDVI changes over March 2000 to September 2012 and March 2000 to December 2018 in the study region were 0.0032 and 0.00243 per month, respectively. These results implied the larger spatial extent and higher magnitude of greening trend from March 2000 to September 2012 compared with those of the entire study period. For the entire study period, it is noteworthy that there were still many parts ($\sim 39.30\%$) of the study region with significant greening trends, even though no statistically significant trend was observed across the whole study region. The implication of this result is that regional greening could be masked by the overall trend, and detailed changes in greenness observed at a fine spatial scale should be considered for vegetation trend estimations.

The greening trends in the inland were stronger than that in the coastal area from March 2000 to September 2012 (Figure 4a). For the entire study period, however, most of vegetation in the inland did not show significant trend, whereas the significant greening trends could still be detected in the coastal area (Figure 4b). The spatial patterns of vegetation change trends in the second segment in Figure S2 showed negative vegetation trends in parts of the inland areas. These areas of negative vegetation trends in the second segment can offset the greening trend during the first segment and result in negative vegetation trends in the entire study period. These results reveal that the greenness trends in the study region have distinct spatial variabilities over different time periods.

4 | DISCUSSION

As shown in Figure 2, large monthly precipitation events, such as April 2001, February 2002, April 2006, March 2008, January 2011 to May 2011, March 2012 and March 2013, induced the increases in greenness about 2 months later. This result implied that increases in vegetation greenness were associated with the occurrence of large precipitation event in this region. These large precipitation events could result in infiltration into deeper soil layers protected from surface evaporation, and the stored precipitation can support vegetation growth later (Lehmann et al., 2019). Moreover, the relatively humid conditions after the heavy precipitation enable most of plant seeds (e.g., *S. sabulicola* and *T. hereroensis*) to germinate (Seely, 1990), and then low precipitation and other water resources (e.g., fog and dew) could support these new plants to survive in the extremely arid environment of the Namib Desert (Ebner et al., 2011; Kaseke et al., 2017; Qiao et al., 2020). The results of annual extreme precipitation amount and the number of extreme precipitation events shown in Figure 5 indicated that extreme precipitation with precipitation above the 95% percentile (0.0309 mm/h) can stimulate vegetation growth. It is noteworthy that the increased NDVI in 2011 without extreme precipitation events could also be related to heavy precipitation events,

because there were heavy rainfall events that occurred during five consecutive months (from January to May) in 2011 with the precipitation greater than the 87% percentile (0.0184 mm/h). The distribution of monthly precipitation over the study period was presented in Figure S1. In addition, the average annual frequency of extreme precipitation events during 2000 to 2012 is 0.0705, while the value is 0.0139 from 2012 to 2018. These results suggest that extreme precipitation events play a role in the long-term vegetation greening trends in the study region. This study also explored trends of precipitation time series shown in Figure 2 using Mann–Kendall test. However, no significant increased trends in precipitation were found during both March 2000 to September 2012 and March 2000 to December 2018. The SEM results (Figure 3) revealed the positive trends in NDVI over March 2000 to September 2012, which could be primarily attributed to CO₂ concentration and precipitation. These results indicated that precipitation was still a main positive driver of vegetation greening in this area even though it did not present increasing trends. This finding is different from previous studies which suggested that increasing precipitation trend was the main reason of observed greening trends in many drylands like Sahel and southern Africa (Fensholt et al., 2012; Hickler et al., 2005; Zhu et al., 2016). The results in our study implied that intensity and frequency of extreme precipitation should also be considered in the investigation about the effect of precipitation on vegetation trends in drylands.

Elevated atmospheric CO₂ concentration was another main driver of observed greening trends in the study area (Figure 3). On the one hand, CO₂ fertilisation effects, caused by increased levels of atmospheric CO₂ concentration, can enhance plant growth by accelerating the rate of photosynthesis (Farquhar & Sharkey, 1982). On the other hand, rising atmospheric CO₂ concentration can induce decreases in leaf stomatal conductance and increase plant water use efficiency (Keenan et al., 2013; Lu, Wang, & McCabe, 2016). More soil water could be remained under the same productivity levels through increasing water use efficiency (Donohue et al., 2013; Lu, Wang, & McCabe, 2016) and is expected to positively affect vegetation greenness particularly over arid regions constrained by water availability. The negative effect of CO₂ in the nonsignificant vegetation trend during the second segment (Figure 2) could result from the phenomenon of structural overshoot (Jump et al., 2017), a process of increased aboveground biomass development due to more favourable water availability in the past and the consequent temporal mismatch between water availability and demand. The favourable precipitation condition in the first segment could stimulate vegetation growth and lead to high water use, thereby increasing drought stress and plant mortality associated with competition for limited soil water resources under the lower precipitation condition of the second segment (Yu et al., 2019; Zhang et al., 2021). The increasing drought stress and plant mortality could offset any positive plant-growth effects of CO₂ fertilisation in the second segment (Jump et al., 2017).

About 75% of the study region experienced significant greening during March 2000 to September 2012, while the proportion of greening areas in the entire study period decreased to 39.30% (Figure 4). To illustrate the reason of lower greening trend in the

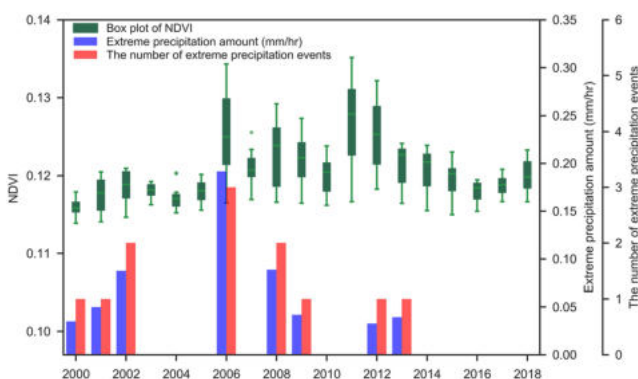


FIGURE 5 The distribution of annual Normalized Difference Vegetation Index (NDVI) values, the annual extreme precipitation amount and the number of extreme precipitation events from 2000 to 2018 for the study region outlined in Figure 1

entire study period, this study calculated the percentage change in precipitation before (March 2000 to September 2012) and after the break point (October 2012 to December 2018) (Figure 6). The result revealed that most of the study region showed a substantial reduction in precipitation after the break point and the average pixel-wise percentage change in precipitation was -38.16% . Since precipitation is a key driver of vegetation greening in this study region, the reduction in precipitation over October 2012 to December 2018 could account for the lower greening trend observed in the entire study period compared with the greening in March 2000 to September 2012. Moreover, the area of negative vegetation trends in the entire study period concentrated in the north of the Namib Sand Sea is larger than that during March 2000 to September 2012. As the diminished precipitation in the north area of this study region (Figure 6) after the breakpoint, the larger area of negative vegetation trend in the entire study period than that in the period of March 2000 to September 2012 could be associated with the low water input over October 2012 to December 2018.

The significant vegetation greening distribution, especially in the northern area of the study region, exhibited a line-shaped feature (e.g., the ripple shape of sand dune) (Figure 4). The line-shaped feature could be observed in the spatial patterns of averaged NDVI (Figure 7)

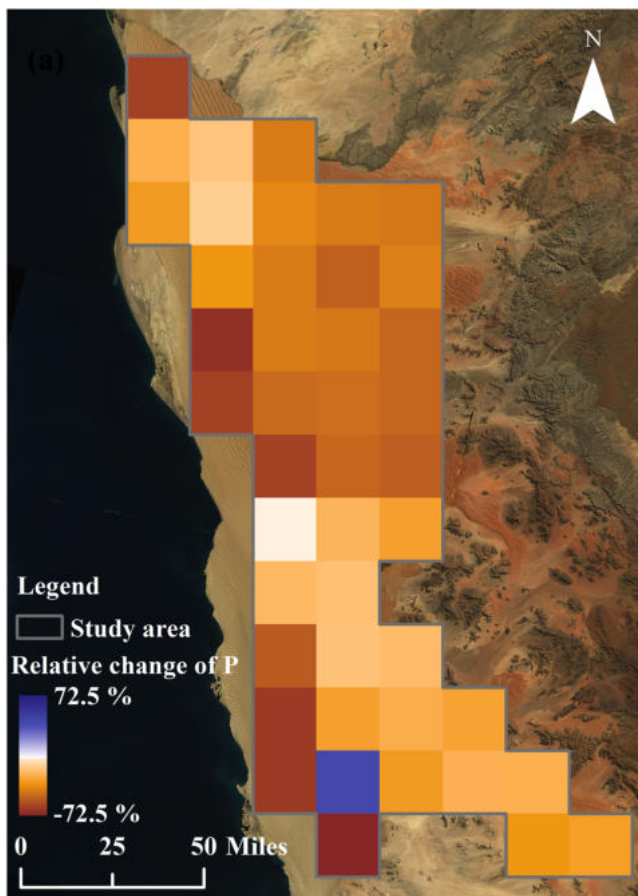


FIGURE 6 The percentage change in precipitation before (March 2000 to September 2012) and after the break point (October 2012 to December 2018) in the study area

as well. This spatial feature of greening might be attributed to the morphology features of sand dunes and characteristics of vegetation coverage caused by the complex moisture gradient in dune slopes. There are distinct dune morphology patterns in the Namib Sand Sea: transverse dunes in the west, linear dunes in the centre and star dunes in the east (Livingstone, 2013). Previous studies suggest that vegetation coverage at the middle of dune slopes is much higher than that at dune base and interdune areas, while the top areas of dune with the maximum rate of sand movement are largely devoid of vegetation (Ronca et al., 2015; Seely, 1990; Yeaton, 1988). Thus, the linear sand dunes and relatively high vegetation coverage on dune slopes could form the line-shapes pattern in the greening distributions.

The greening trend in the inland of the study region was strikingly stronger than that in the coastal zone during March 2000 to September 2012 (Figure 4a), which indicated that the greening rate of vegetation in the inland was obviously faster than the coastal zone during the first segment. We also found the similar spatial patterns in averaged NDVI for both the first segment and the entire study period (Figure 7)—vegetation greenness increasing from the coastal zone to the inland. These results indicated that the greening rate was generally faster in denser vegetated areas during the first segment, the period with relatively higher frequency of extreme precipitation events compared with the entire study period. In turn, the gradient of vegetation greening rate from the coastal zone to the inland could increase spatial heterogeneity in vegetation greenness in the study region.

Over March 2000 to December 2018, the large coherent areas with greening trends were observed in the coastal area in Figure 4b. It could result from fog water input (Lancaster et al., 1984). Since the typical plant species in this study area, such as *S. sabulicola* and *T. hereroensis*, can survive by taking up fog water through leaves or shallow roots (Ebner et al., 2011; Wang et al., 2019), fog water can be an important water supply for vegetation growth under the prolonged low precipitation condition (Adhikari & Wang, 2020; Li et al., 2018; Qiao et al., 2020; Wang et al., 2017). Previous studies suggested that the mean amount of fog water for the northern Namib Sea Sand increased from 34 mm per year in the coast to a maximum of 184 mm 35- to 60-km inland and decreased sharply thereafter to 15 mm or less in the east of the desert (Lancaster et al., 1984). Other findings indicated that the southwest region received quite regular fog events due to the upwelling Benguela Current of the southern African coast (Ebner et al., 2011). These regular fogs in the coastal zone could improve plant water stress and maintain vegetation function in the low precipitation period (October 2012 to December 2018). In addition, since the effects of temperature on plant growth are negative in the study region (Figure 3), the cool temperature in the coastal zone, relative to the hotter inland area (Lancaster et al., 1984; Lancaster, 2002), might reduce heat stress on vegetation growth in the coastal zone. Thus, the divergent greening patterns in the coastal zone and inland areas during the entire study period might be associated with the higher fog water input and lower temperature in the coastal zone.

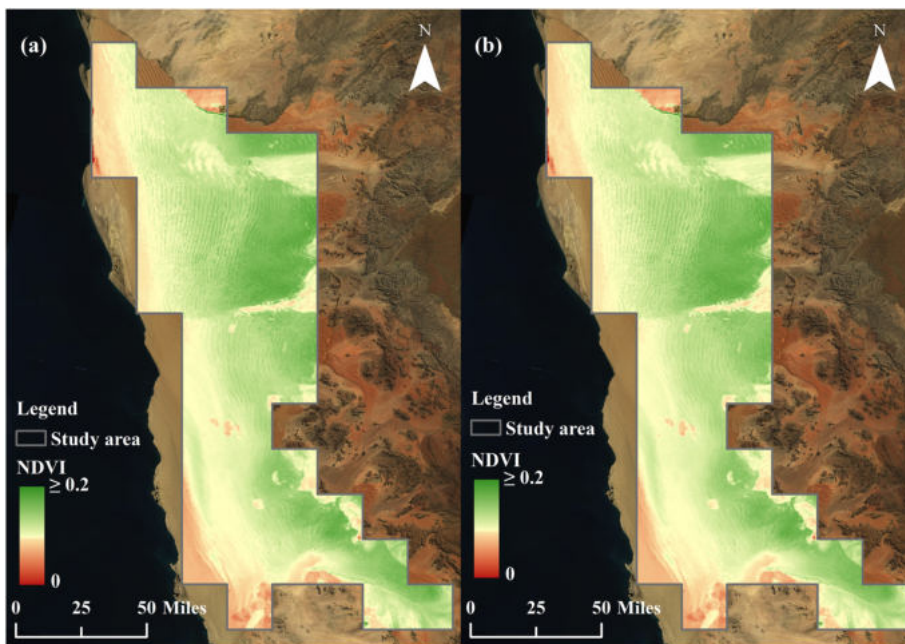


FIGURE 7 Spatial patterns of average vegetation greenness derived from monthly mean Moderate Resolution Spectroradiometer (MODIS) Normalized Difference Vegetation Index (NDVI) for time periods of March 2000 to September 2012 (a) and March 2000 to December 2018 (b) in the study area

Other factors might also affect the vegetation greening in the study region, such as dew water, mineral content gradient. It has been reported that dew water could improve plant water status in the arid environment (Wang et al., 2019). Variations in iron oxide and clay minerals from inland to coastal regions generated a pattern of red sands in the east, grading into yellowish brown sands in the west (White et al., 2007). This mineral content gradient from inland to coastal regions might affect vegetation growth (Fink et al., 2016).

This study identified the regional greening in the Namib sand sea without direct human activities and shrub expansion using the high-quality MODIS dataset and explored its potential driving factors including precipitation, temperature and CO_2 . The results suggested that the significant greening trends were mainly driven by precipitation and increasing atmospheric CO_2 concentration in the study region. Especially, the amount and frequency of extreme precipitation could be important hydrological variables in understanding the effect of precipitation on vegetation trends in drylands.

5 | CONCLUSION

Our research examines the vegetation greening trend in the Namib Sand Sea. This study complements previous studies for greening trends in many drylands influenced by direct human activities and species composition changes (e.g., shrub encroachment). The study region exhibited significant greening trends over 2000 to 2012, primarily driven by precipitation and increasing atmospheric CO_2 concentration. Warming could reduce plant growth in the study region, which was inferred from the negative effects of temperature on greenness. The amount of extreme precipitation, rather than the trend of

precipitation, seems to play an important role in the observed greening trends. This finding is different from the previous studies which suggested that increasing precipitation trend was one main reason for greening in many drylands. These results imply, apart from the precipitation trend, that intensity and frequency of extreme precipitation should be also considered in future investigations about vegetation greening in drylands.

Spatially, about 75% of the study region was undergoing a statistically significant greening trend from March 2000 to September 2012, and the value decreased to 39.30% for 2000 to 2018 mainly caused by the reduction in precipitation after 2012. The greening trend presented distinct spatial variability over different study periods, such as higher greening rate in the inland than the coastal area for 2000 to 2012 and significant greening trends in the coastal area over 2000 to 2018. These pronounced spatial features in greening distribution over different study periods might be related to spatial variations in vegetation density and fog water in the study region. The different vegetation trend results between the entire study region and the pixel scale patterns over 2000 to 2018 implied that significant changes in greenness could be masked if only average value was used for a large region. This study fills an important knowledge gap of vegetation dynamics in regions without direct human activities. Our findings significantly improve the understanding of the contributions of climate factors to vegetation dynamics and the spatial feature of vegetation greening in the Namib Sand Sea.

ACKNOWLEDGEMENTS

We thank five anonymous reviewers for the constructive comments, and these comments significantly improved the quality of the manuscript. We acknowledge the funding support of the National Science Foundation grant (EAR-1554894).

CONFLICT OF INTEREST

The authors declare that they have no known competing financial interests or personal relationships that could have appeared to influence the work reported in this paper.

SIGNIFICANCE STATEMENT

The analyses of greenness trend for regions without direct human activities in drylands are lacking. This study investigates the vegetation trend across the Namib sand sea between 2000 and 2018 using monthly satellite observations and examines several potential driving factors. We found that the study region exhibited significant greening trends over 2000 to 2012 but not over 2012 to 2018. Warming reduced plant growth in the study region. The amount of heavy precipitation, rather than the trend of precipitation, seems to play an important role in the observed greening trends. Our findings fill an important knowledge gap of vegetation dynamics in regions without direct human activities.

DATA AVAILABILITY STATEMENT

MCD43A4 and MCD43A2 data were available from the Land Processes Distributed Active Archive Center (<https://lpdaac.usgs.gov/products/mcd43a4v006/>). Tropical Rainfall Measuring Mission precipitation product (TRMM 3B43) was obtained from the Goddard Earth Sciences Data and Information Services Center (GES DISC) (https://disc2.gesdisc.eosdis.nasa.gov/opendap/TRMM_L3/TRMM_3B43.7/). The temperature data were derived from the European Centre for Medium Range Weather Forecasts reanalysis dataset (ERA5) (<https://cds.climate.copernicus.eu/cdsapp#!/dataset/reanalysis-era5-land-monthly-means>). The CO₂ concentration data were obtained from the Global Monitoring Division of National Oceanic and Atmospheric Administration (NOAA) Earth System Research Laboratory (<https://www.esrl.noaa.gov/gmd/ccgg/trends/global.html>).

REFERENCES

- Adhikari, B., & Wang, L. (2020). The potential contribution of soil moisture to fog formation in the Namib Desert. *Journal of Hydrology*, 591, 125326. <https://doi.org/10.1016/j.jhydrol.2020.125326>
- Ambika, A. K., Wardlow, B., & Mishra, V. (2016). Remotely sensed high resolution irrigated area mapping in India for 2000 to 2015. *Scientific Data*, 3(1), 1–14. <https://doi.org/10.1038/sdata.2016.118>
- Ballantyne, A. P., Alden, C. B., Miller, J. B., Tans, P. P., & White, J. W. C. (2012). Increase in observed net carbon dioxide uptake by land and oceans during the past 50 years. *Nature*, 488(7409), 70–72. <https://doi.org/10.1038/nature11299>
- Boker, S. M., Rotondo, J. L., Xu, M., & King, K. (2002). Windowed cross-correlation and peak picking for the analysis of variability in the association between behavioral time series. *Psychological Methods*, 7(3), 338–355. <https://doi.org/10.1037/1082-989X.7.3.338>
- Bonan, G. B., Pollard, D., & Thompson, S. L. (1992). Effects of boreal forest vegetation on global climate. *Nature*, 359(6397), 716–718. <https://doi.org/10.1038/359716a0>
- Chen, C., Park, T., Wang, X., Piao, S., Xu, B., Chaturvedi, R. K., Fuchs, R., Brovkin, V., Ciais, P., Fensholt, P., Tømmervik, H., Bala, G., Zhu, Z., Nemani, R. R., & Myneni, R. B. (2019). China and India lead in greening of the world through land-use management. *Nat Sustain*, 2(2), 122–129. <https://doi.org/10.1038/s41893-019-0220-7>
- D'Oodorico, P., Laio, F., Porporato, A., Ridolfi, L., Rinaldo, A., & Rodriguez-Iturbe, I. (2010). Ecohydrology of terrestrial ecosystems. *Bioscience*, 60(11), 898–907. <https://doi.org/10.1525/bio.2010.60.11.6>
- Donohue, R. J., Roderick, M. L., McVicar, T. R., & Farquhar, G. D. (2013). Impact of CO₂ fertilization on maximum foliage cover across the globe's warm, arid environments. *Geophysical Research Letters*, 40(12), 3031–3035. <https://doi.org/10.1002/grl.50563>
- Ebner, M., Miranda, T., & Roth-Nebelsick, A. (2011). Efficient fog harvesting by *Stipagrostis sabulicola* (Namib dune bushman grass). *Journal of Arid Environments*, 75(6), 524–531. <https://doi.org/10.1016/j.jaridenv.2011.01.004>
- Eldridge, D. J., Wang, L., & Ruiz-Colmenero, M. (2015). Shrub encroachment alters the spatial patterns of infiltration. *Ecohydrology*, 8(1), 83–93. <https://doi.org/10.1002/eco.1490>
- Farquhar, G. D., & Sharkey, T. D. (1982). Stomatal conductance and photosynthesis. *Annual Review of Plant Physiology*, 33(1), 317–345. <https://doi.org/10.1146/annurev.pp.33.060182.001533>
- Fensholt, R., Langanke, T., Rasmussen, K., Reenberg, A., Prince, S. D., Tucker, C., Scholes, R. J., Bao Le, Q., Bondeau, A., Eastman, R., Epstein, H., Gaughan, A. E., Hellden, U., Mbow, C., Olsson, L., Paruelo, J., Schweitzer, C., Seaquist, J., & Wessels, K. (2012). Greenness in semi-arid areas across the globe 1981–2007 – An earth observing satellite based analysis of trends and drivers. *Remote Sensing of Environment*, 121, 144–158. <https://doi.org/10.1016/j.rse.2012.01.017>
- Fensholt, R., Rasmussen, K., Kaspersen, P., Huber, S., Horion, S., & Swinnen, E. (2013). Assessing land degradation/recovery in the African Sahel from long-term earth observation based primary productivity and precipitation relationships. *Remote Sensing*, 5(2), 664–686. <https://doi.org/10.3390/rs5020664>
- Fink, J. R., Inda, A. V., Tiecher, T., & Barrón, V. (2016). Iron oxides and organic matter on soil phosphorus availability. *Ciencia e Agrotecnologia*, 40(4), 369–379. <https://doi.org/10.1590/1413-70542016404023016>
- Gilbert, N. (2011). Science enters desert debate: United Nations considers creating advisory panel on land degradation akin to IPCC. *Nature*, 477(7364), 262. <https://doi.org/10.1038/477262a>
- Grace, J. B. (2006). *Structural Equation Modeling and Natural Systems*. Cambridge University Press. <https://doi.org/10.1017/CBO9780511617799>
- Griscom, B. W., Adams, J., Ellis, P. W., Houghton, R. A., Lomax, G., Miteva, D. A., Schlesinger, W. H., Shoch, D., Siikamäki, J. V., Smith, P., Woodbury, P., Zganjar, C., Blackman, A., Campari, J., Conant, R. T., Delgado, C., Elias, P., Gopalakrishna, T., Hamsik, M. R., ... Fargione, J. (2017). Natural climate solutions. *Proceedings of the National Academy of Sciences*, 114(44), 11645–11650. <https://doi.org/10.1073/pnas.1710465114>
- Helldén, U., & Tottrup, C. (2008). Regional desertification: A global synthesis. *Global and Planetary Change*, 64(3–4), 169–176. <https://doi.org/10.1016/j.gloplacha.2008.10.006>
- Herrmann, S. M., Anyamba, A., & Tucker, C. J. (2005). Recent trends in vegetation dynamics in the African Sahel and their relationship to climate. *Global Environmental Change*, 15(4), 394–404. <https://doi.org/10.1016/j.gloenvcha.2005.08.004>
- Hickler, T., Eklundh, L., Seaquist, J. W., Smith, B., Ardö, J., Olsson, L., Sykes, M. T., & Sjöström, M. (2005). Precipitation controls Sahel greening trend. *Geophysical Research Letters*, 32(21), L21415. <https://doi.org/10.1029/2005GL024370>
- Hoyle, R. H. (1995). The structural equation modeling approach: Basic concepts and fundamental issues. In *Structural Equation Modeling: Concepts, Issues, and Applications* (pp. 1–15). Sage Publications, Inc.
- Jiao, W., Wang, L., & McCabe, M. F. (2021). Multi-sensor remote sensing for drought characterization: Current status, opportunities and a roadmap for the future. *Remote Sensing of Environment*, 256, 112313. <https://doi.org/10.1016/j.rse.2021.112313>

- Jiao, W., Wang, L., Smith, W. K., Chang, Q., Wang, H., & D'Odorico, P. (2021). Observed increasing water constraint on vegetation growth over the last three decades. *Nature Communications*, 12, 3777. <https://doi.org/10.1038/s41467-021-24016-9>
- Jump, A. S., Ruiz-Benito, P., Greenwood, S., Allen, C. D., Kitzberger, T., Fensham, R., Martínez-Vilalta, J., & Lloret, F. (2017). Structural overshoot of tree growth with climate variability and the global spectrum of drought-induced forest dieback. *Global Change Biology*, 23(9), 3742–3757. <https://doi.org/10.1111/gcb.13636>
- Kaseke, K. F., Wang, L., & Seely, M. K. (2017). Nonrainfall water origins and formation mechanisms. *Science Advances*, 3(3), e1603131. <https://doi.org/10.1126/sciadv.1603131>
- Keenan, T. F., Hollinger, D. Y., Bohrer, G., Dragoni, D., Munger, J. W., Schmid, H. P., & Richardson, A. D. (2013). Increase in forest water-use efficiency as atmospheric carbon dioxide concentrations rise. *Nature*, 499(7458), 324–327. <https://doi.org/10.1038/nature12291>
- Lal, R. (2004). Carbon sequestration in dryland ecosystems. *Environmental Management*, 33(4), 528–544. <https://doi.org/10.1007/s00267-003-9110-9>
- Lancaster, J., Lancaster, N., & Seely, M. (1984). Climate of the central Namib Desert. *Madoqua*, 14(1), 5–61. https://doi.org/10.10520/AJA10115498_484
- Lancaster, N. (2002). How dry was dry?—Late Pleistocene palaeoclimates in the Namib Desert. *Quaternary Science Reviews*, 21(7), 769–782. [https://doi.org/10.1016/S0277-3791\(01\)00126-3](https://doi.org/10.1016/S0277-3791(01)00126-3)
- Lanning, M., Wang, L., Scanlon, T. M., Vadeboncoeur, M. A., Adams, M. B., Epstein, H. E., & Druckenbrod, D. (2019). Intensified vegetation water use under acid deposition. *Science Advances*, 5(7), eaav5168. <https://doi.org/10.1126/sciadv.aav5168>
- Lehmann, P., Berli, M., Koonce, J. E., & Or, D. (2019). Surface evaporation in arid regions: Insights from lysimeter decadal record and global application of a surface evaporation capacitor (SEC) model. *Geophysical Research Letters*, 46(16), 9648–9657. <https://doi.org/10.1029/2019GL083932>
- Li, B., Wang, L., Kaseke, K. F., Vogt, R., Li, L., & Seely, M. (2018). The impact of fog on soil moisture dynamics in the Namib Desert. *Advances in Water Resources*, 113, 23–29. <https://doi.org/10.1016/j.advwatres.2018.01.004>
- Liu, Y. Y., Van Dijk, A. I. J. M., McCabe, M. F., Evans, J. P., & De Jeu, R. A. M. (2013). Global vegetation biomass change (1988–2008) and attribution to environmental and human drivers. *Global Ecology and Biogeography*, 22(6), 692–705. <https://doi.org/10.1111/geb.12024>
- Livingstone, I. (2013). Aeolian geomorphology of the Namib sand sea. *Journal of Arid Environments*, 93, 30–39. <https://doi.org/10.1016/j.jaridenv.2012.08.005>
- Lu, X., & Wang, L. (2019). Evaluating ecohydrological modelling framework to link atmospheric CO₂ and stomatal conductance. *Ecohydrology*, 12(1), e2051. <https://doi.org/10.1002/eco.2051>
- Lu, X., Wang, L., & McCabe, M. F. (2016). Elevated CO₂ as a driver of global dryland greening. *Scientific Reports*, 6(1), 20716. <https://doi.org/10.1038/srep20716>
- Lu, X., Wang, L., Pan, M., Kaseke, K. F., & Li, B. (2016). A multi-scale analysis of Namibian rainfall over the recent decade—Comparing TMPA satellite estimates and ground observations. *Journal of Hydrology: Regional Studies*, 8, 59–68. <https://doi.org/10.1016/j.ejrh.2016.07.003>
- Muñoz Sabater, J. (2019). ERA5-Land monthly averaged data from 1981 to present. In *Copernicus Climate Change Service (C3S) Climate Data Store (CDS)*. <https://doi.org/10.24381/cds.68d2bb3>
- Olsson, L., Eklundh, L., & Arđö, J. (2005). A recent greening of the Sahel—Trends, patterns and potential causes. *Journal of Arid Environments*, 63(3), 556–566. <https://doi.org/10.1016/j.jaridenv.2005.03.008>
- Pausata, F. S. R., Gaetani, M., Messori, G., Berg, A., De Souza, M. D., Sage, R. F., & deMenocal, P. B. (2020). The greening of the Sahara: Past changes and future implications. *One Earth*, 2(3), 235–250. <https://doi.org/10.1016/j.oneear.2020.03.002>
- Pfeifer, M., Disney, M., Quaife, T., & Marchant, R. (2012). Terrestrial ecosystems from space: A review of earth observation products for macroecology applications. *Global Ecology and Biogeography*, 21(6), 603–624. <https://doi.org/10.1111/j.1466-8238.2011.00712.x>
- Piao, S., Wang, X., Park, T., Chen, C., Lian, X., He, Y., Bjerke, J. W., Chen, A., Ciais, P., Tømmervik, H., Nemani, R. R., & Myneni, R. B. (2020). Characteristics, drivers and feedbacks of global greening. *Nature Reviews Earth & Environment*, 1(1), 14–27. <https://doi.org/10.1038/s43017-019-0001-x>
- Piao, S., Yin, G., Tan, J., Cheng, L., Huang, M., Li, Y., Liu, R., Mao, J., Myneni, R. B., Peng, S., Poulter, B., Shi, X., Xiao, Z., Zeng, N., Zeng, Z., & Wang, Y. (2015). Detection and attribution of vegetation greening trend in China over the last 30 years. *Global Change Biology*, 21(4), 1601–1609. <https://doi.org/10.1111/gcb.12795>
- Qiao, N., Zhang, L., Huang, C., Jiao, W., Maggs-Kölling, G., Marais, E., & Wang, L. (2020). Satellite observed positive impacts of fog on vegetation. *Geophysical Research Letters*, 47(12), e2020GL088428. <https://doi.org/10.1029/2020gl088428>
- Ronca, S., Ramond, J.-B., Jones, B., Seely, M., & Cowan, D. (2015). Namib Desert dune/interdune transects exhibit habitat-specific edaphic bacterial communities. *Frontiers in Microbiology*, 6, 845. <https://doi.org/10.3389/fmicb.2015.00845>
- Saha, M. V., Scanlon, T. M., & D'Odorico, P. (2015). Examining the linkage between shrub encroachment and recent greening in water-limited southern Africa. *Ecosphere*, 6(9), 156. <https://doi.org/10.1890/es15-00098.1>
- Schaaf, C., & Wang, Z. (2015). MCD43A3 MODIS/Terra+Aqua BRDF/Albedo Nadir BRDF Adjusted Ref Daily L3 Global - 500m V006 [Data set]. In *NASA EOSDIS Land Processes DAAC*. <https://doi.org/10.5067/MODIS/MCD5043A5064.5006>
- Seely, M. K. (1990). Patterns of plant establishment on a linear desert dune. *Israel Journal of Plant Sciences*, 39(4), 443–451. <https://doi.org/10.1080/0021213X.1990.10677167>
- Sen, P. K. (1968). Estimates of the regression coefficient based on Kendall's tau. *Journal of the American Statistical Association*, 63(324), 1379–1389. <https://doi.org/10.1080/01621459.1968.10480934>
- Seveviratne, S., Nicholls, N., Easterling, D., Goodess, C. M., Kanae, S., Kossin, J., Luo, Y., Marengo, J., McInnes, K., Rahimi, M., Reichstein, M., Sorteberg, A., Vera, C., Zhang, X., & Rahlmi, M. (2012). Changes in climate extremes and their impacts on the natural physical environment. In *Managing the Risks of Extreme Events and Disasters to Advance Climate Change Adaptation: Special Report of the Intergovernmental Panel on Climate Change* (pp. 109–230). Cambridge University Press. <https://doi.org/10.1017/CBO9781139177245.006>
- Theil, H. (1950). A rank-invariant method of linear and polynomial regression analysis. *Indagationes Mathematicae*, 12(85), 173–177.
- Tian, F., Brandt, M., Liu, Y. Y., Rasmussen, K., & Fensholt, R. (2017). Mapping gains and losses in woody vegetation across global tropical drylands. *Global Change Biology*, 23(4), 1748–1760. <https://doi.org/10.1111/gcb.13464>
- TRMM. (2011). Tropical rainfall measuring mission (TRMM) (TMPA/3B43) rainfall estimate L3 1 month 0.25 degree x 0.25 degree V7. In *Earth Sciences Data and Information Services Center (GES DISC)*. <https://doi.org/10.5067/TRMM/TMPA/MONTH/5067>
- Wang, L., D'Odorico, P., Evans, J., Eldridge, D., McCabe, M., Caylor, K., & King, E. (2012). Dryland ecohydrology and climate change: Critical issues and technical advances. *Hydrology and Earth System Sciences*, 16(8), 2585–2603. <https://doi.org/10.5194/hess-16-2585-2012>
- Wang, L., Good, S. P., & Caylor, K. K. (2014). Global synthesis of vegetation control on evapotranspiration partitioning. *Geophysical Research Letters*, 41(19), 6753–6757. <https://doi.org/10.1002/2014GL061439>
- Wang, L., Kaseke, K. F., Ravi, S., Jiao, W., Mushi, R., Shuuya, T., & Maggs-Kölling, G. (2019). Convergent vegetation fog and dew water use in

- the Namib Desert. *Ecohydrology*, 12(7), e2130. <https://doi.org/10.1002/eco.2130>
- Wang, L., Kaseke, K. F., & Seely, M. K. (2017). Effects of non-rainfall water inputs on ecosystem functions. *Wiley Interdisciplinary Reviews: Water*, 4(1), e1179. <https://doi.org/10.1002/wat2.1179>
- White, K., Walden, J., & Gurney, S. D. (2007). Spectral properties, iron oxide content and provenance of Namib dune sands. *Geomorphology*, 86(3–4), 219–229. <https://doi.org/10.1016/j.geomorph.2006.08.014>
- Yeaton, R. (1988). Structure and function of the Namib dune grasslands: Characteristics of the environmental gradients and species distributions. *The Journal of Ecology*, 76(3), 744–758. <https://doi.org/10.2307/2260571>
- Yu, K., & D'Odorico, P. (2014). An ecohydrological framework for grass displacement by woody plants in savannas. *Journal of Geophysical Research: Biogeosciences*, 119(3), 192–206. <https://doi.org/10.1002/2013JG002577>
- Yu, K., Smith, W. K., Trugman, A. T., Condit, R., Hubbell, S. P., Sardans, J., Peng, C., Zhu, K., Peñuelas, J., Cailleret, M., Levanic, T., Gessler, A., Schaub, M., Ferretti, M., & Anderegg, W. R. L. (2019). Pervasive decreases in living vegetation carbon turnover time across forest climate zones. *Proceedings of the National Academy of Sciences*, 116(49), 24662–24667. <https://doi.org/10.1073/pnas.1821387116>
- Zhang, Y., Keenan, T. F., & Zhou, S. (2021). Exacerbated drought impacts on global ecosystems due to structural overshoot. *Nat Ecol Evol*, 5(11), 1490–1498. <https://doi.org/10.1038/s41559-021-01551-8>
- Zhu, Z., Piao, S., Myneni, R. B., Huang, M., Zeng, Z., Canadell, J. G., Ciais, P., Sitch, S., Friedlingstein, P., Arneeth, A., Cao, C., Cheng, L., Kato, E., Koven, C., Li, Y., Lian, X., Liu, Y., Liu, R., Mao, J., ... Zeng, N. (2016). Greening of the earth and its drivers. *Nature Climate Change*, 6(8), 791–795. <https://doi.org/10.1038/nclimate3004>

SUPPORTING INFORMATION

Additional supporting information may be found in the online version of the article at the publisher's website.

How to cite this article: Qiao, N., & Wang, L. (2022). Satellite observed vegetation dynamics and drivers in the Namib sand sea over the recent 20 years. *Ecohydrology*, e2420. <https://doi.org/10.1002/eco.2420>